

# ***I-V Characteristics Measuring System for PV Generator based on PDM Inverter***

A. Sandali<sup>1</sup> and A. Cheriti<sup>2</sup>

<sup>1</sup> Department of Electrical Engineering  
ENSEM., Hassan II Casablanca University  
Boulevard Abdellah Ibrahim (Ex. Route d'El Jadida), 20200 Casablanca (Morocco)  
Phone/Fax number: +00212 522 230789, e-mail: sandali@uqtr.ca

<sup>2</sup> Department of Electrical and Computer Engineering Université du Québec à Trois-Rivières  
3351, boulevard des Forges, Trois-Rivières (Québec) G8Z 4M3, Canada  
Phone, fax : +00 819 376-5011, e-mail : Cheriti@uqtr.ca

**Abstract.** This paper presents a new method to characterize photovoltaic panels. The power electronic converter used is a Pulse Density Modulation (PDM) inverter. In this method, the inverter plays two roles: First, it is a DC inductor emulator. Second, it allows assembly between inductive and capacitive load methods. The PDM inverter is adapted to operate at very high switching frequency. In this application, it avoids the difficulties of making DC inductors with high DC current and its control remains very simple. This is an asset for increasing the power, power density and rapidity of tracers based on this method. The main disadvantage of this method, compared to methods based on DC-DC converter, is the use of twice as many semiconductor components. But this disadvantage can be compensated by a gain on reactive components. The simulations and experimental results of the proposed system are shown.

**Key words.** PV generator, PDM inverter, I-V curve tracer, DC inductor emulator

## **1. Introduction**

PV production is experiencing great extraordinary development from all points of view. PV module cost fell from 105.7 USD per watt in 1975 to 0.2 USD per watt in 2020 [1]. In 2010, PV installed capacity was less than 20 GW. In 2020, it is multiplied by about seven to reach a cumulative capacity of 760 GW [2] and PV generation increased 156 TWh to reach 821 TWh. This represents an annual growth rate of 23% [3]. In 2021, PV electricity was supposed to increase by 145 TWh to approach 1000 TWh, i.e. a growth rate of 18% [4]. During the same year, 183 GW have been installed in 2021 and cumulative capacity has become very close to the 1 TW mark [5]. However, the world expects more. The Net Zero Emission (NZE) by 2050 scenario forecasts for PV production at an annual growth rate of 24% between 2020 and 2030 and the annual installation of 630 GW to reach 6970 TWh in 2030 [6]. The cumulative installed capacity of PV must be 20 times greater in 2050 [6]. These predictions are consistent with those of IRENA's Remap analysis [7].

Given the development prospects, the research activity is very intense in the PV production field and concerns all its aspects. I-V curve tracing is one of the aspects concerned. During their life cycle, the performance of PV generators may experience various degradations [8, 9]. The I-V curve is a radiography of their state of health. To ensure optimal operation, it is essential to have the equipment to trace the I-V curves of the PV generators under real operating conditions. The I-V curves given by the manufacturers remain indicative. Various methods are used in I-V solar tracers [10-13]. A first categorization of I-V tracers can be made, depending on whether climate data sensors are used. IV tracers without climatic sensors are best suited to the needs and expectations of designers and operators of photovoltaic production systems. In this category, tracers are based on inductive, capacitive or resistive load methods. Among those based on the resistive load method, some use a real variable resistor and others use variable resistor emulators. The latter is based on power transistors used as ballast [14, 15] or based on DC-DC converters [13, 16]. All these methods are confronted with conceptual and/or technological limitations. To enrich and diversify the characterization methods of PV generators, the work presented introduces Pulse Density Modulation in the PV production field. PDM control is based on the soft switching concept. It was introduced in the mid-'90s in induction heating applications [17]. In the mid-2000s, it was extended and adapted to AC-DC-AC conversions with power factor correction and multilevel topology for the DC-AC stage [18] and three-phase configuration for the AC-DC stage [19].

The rest of the paper is organized as follows. Section II presents the principle of I-V tracers based on DC-DC converters and lists the various limitations with which the tracers of this family are confronted. Section III is devoted to the PDM inverter. The operating principle and the theoretical modeling of this type of inverter are presented in this section. Section IV introduces the principle, methodology, and features of the suggested IV tracing technique. In section V, a qualitative analysis is made to

identify potential advancements of the proposed method. Simulation and experimental results are given in section VI and a conclusion is presented in section VII.

## 2. DC-DC Converters in the PV Tracers

In photovoltaic tracer systems, DC-DC converters act as variable resistor emulators. A fixed resistance ( $R_o$ ), placed at the output of the converter, is converted into an equivalent variable resistance seen at the input and is defined by:

$$R_i = R_o/M(\alpha)^2 \quad (1)$$

where  $M$  is the voltage conversion ratio and  $\alpha$  is the duty cycle.

To trace the I-V characteristic of a PV generator, a DC-DC converter can advantageously replace a mechanically variable resistor. However, the option of using a DC-DC converter to trace the IV characteristic of PV generators comes up against conceptual and technological limitations. These limitations are briefly discussed below.

1. The first limitation is that the transformation ratio must be of the buck-boost type (It varies from 0 to infinity) in order to be able to emulate a resistance that varies from 0 to infinity. Only DC-DC converters of the buck-boost type (Buck-boost, Sepic, Cuk, Zeta, ...) can therefore be used to trace the entire characteristic from the point of short circuit to the point of the open circuit or vice versa. The buck and boost type converters are used to trace part of the characteristic.

2. Equation (1), in other words the possibility of considering a DC-DC converter as a resistance controlled by the duty cycle, results from the steady-state converter analysis. The duty cycle must therefore vary very slowly with respect to the switching frequency.

3. Electronic components such as Mosfets, diodes, inductors and capacitors have various imperfections and in particular parasitic resistances. The direct consequence of the latter is that the ratio of transformation cannot be infinite and the input resistance will not reach zero. In the case of the buck-boost, if we take into account the parasitic resistance of the inductance ( $R_L$ ), the conversion ratio becomes:

$$M(\alpha) = (\alpha/(1-\alpha)) \cdot \left(1/\left(1 + \frac{r}{(1-\alpha)^2}\right)\right) \quad (2)$$

where  $r = R_L/R_o$   
its maximum  $M_{max}$  occurs when:

$$\alpha = \alpha_{max} = 1 + r - \sqrt{(1+r)r} \quad (3)$$

If  $r = 3.5\%$ ,  $M_{max} = 2.21$  and  $R_i \geq R_o/5$ . The input resistance is greater than a fifth of the output resistance while theoretically, it must decrease until zero.

4. In the case of a DC inductor, the increase in the rated DC current requires an increase in the effective reluctance of the magnetic circuit. But such action causes a drop in the value of the inductance if the number of turns is not revised upwards. It then appears clearly that keeping the value of the inductance constant and increasing the value of the DC current increases the number of turns and consequently increases the DC resistance. The limitation mentioned above then becomes more important when it comes to characterizing high power panels.

5. The relationship between the resistance seen at the input of a DC-DC converter and the duty cycle is not linear. The equivalent resistance at the input decreases very quickly or very slowly when the duty cycle is close to zero or unity. As

a result, the measured points of the I-V curve are not evenly distributed. In case of shading, the I-V curve may not be drawn with fidelity and local MPPs may be missed.

6. The DC-DC converters used to characterize PV generators are based on the concept of hard switching. The use of HF switching to miniaturize reactive components is limited by the tolerated switching losses.

## 3. PDM Inverter: Principle and Modelling

### A. PDM Control Principle

The Pulse Density Modulation (PDM) was first presented in [17]. It is a type of control applied to a series resonant inverter, which allows power control and lossless switching. Commutations (turn-on and turn-off) occur at zero current. To have such switching, the switching frequency is equal to the resonant frequency of the inverter RLC load. To control the transmitted power, a PDM pattern signal (PDM-P) is introduced: When the PDM pattern is logic high, the inverter switches operate normally. This is the active mode. When the PDM pattern is logic low, the inverter switches open the DC source and short the load. This is the inactive mode. Gate control signals of switches are generated from the PDM pattern and a signal at the resonant frequency (S-Res) by a logic circuit. So that the PDM pattern does not disturb the ZCS operation, it is defined by two parameters (length and duty cycle) subject to constraints:

i) The length of the PDM pattern ( $k$ ) must be a natural number. It represents the number of the load resonance period ( $T_{res}$ ) per PDM pattern period ( $T_{PDMP}$ ):

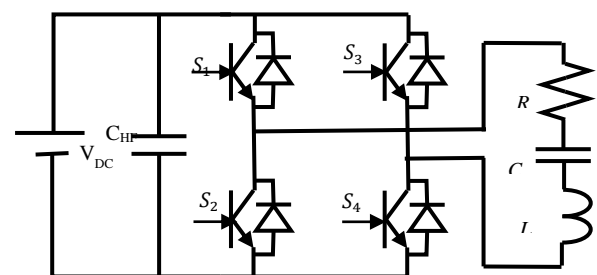
$$k = T_{PDMP}/T_{res} \quad (4)$$

ii) The duty cycle ( $d$ ) must be a rational number and is defined

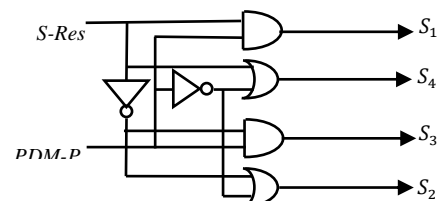
$$d = n/k \quad (5)$$

where  $n = 0, 1, 2, \dots, k$ : number of active cycles per PDM pattern period.

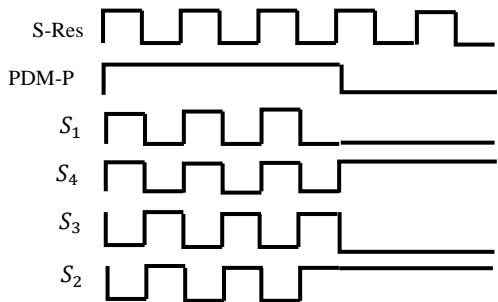
These different aspects are illustrated in Fig. 1.



a) Converter topology



b) Generation of Gate control signals of switches



c) Gate control signals of switches (Case  $k = 5$  and  $d = 3/5$ )  
 Fig. 1. Illustration of the PDM operation

### B. PDM Inverter modeling

PDM inverter modeling is presented in detail in [20]. Here we outline the key points of this modeling. The RLC load damping factor is very low, the load current is then quasi-sinusoidal with a peak value that varies from one period to another because the transient state is considered. Since the output current is sinusoidal and the input current is the rectified form of the first, the calculated peak values are sufficient to determine the output and input currents. This operation is the longest and most delicate in modeling. The capacitor  $C_{HF}$ , placed at the input of the inverter performs a High Frequency (HF) decoupling between the current drawn from the DC source of the inverter and the input current of the inverter. It follows from this decoupling that the current drawn from the DC source is the average, calculated over a half-resonance period, of the input current. Since the latter has a rectified sinusoidal shape, the average calculation is simple. It consists of multiplying the peak values by  $\pi/2$ . The current drawn from the DC source is identified as the current that would be drawn by an equivalent LR load defined by:

$$L_{eq} = L \frac{\pi}{4\xi} \frac{1 - \exp(-\pi\xi\sqrt{1-\xi^2})}{\exp(-\pi\xi\sqrt{1-\xi^2}/2)} \quad (6)$$

$$R_{eq} = R \frac{\pi}{8\xi} \frac{1 - \exp(-\pi\xi\sqrt{1-\xi^2})}{\exp(-\pi\xi\sqrt{1-\xi^2}/2)} \quad (7)$$

where  $\xi$  is the damping factor of RLC load. Figure 2 shows the equivalent DC RL-load vs damping factor of AC RLC-load

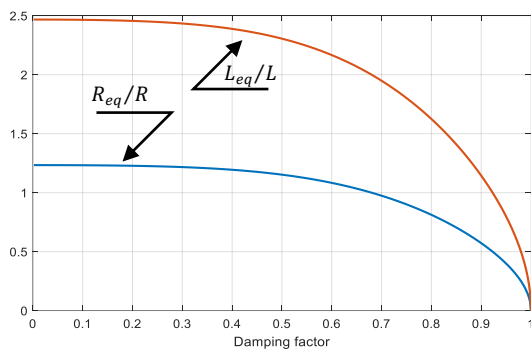


Fig. 2. Elements of equivalent DC load vs damping factor of AC load

The converter can be considered as a buck-fed inverter. The buck is controlled by the PDM pattern and the inverter is controlled by S-Res (Fig. 3). If we are only interested in the current drawn from the DC source, the DC source - PDM inverter association can then be modeled by the DC Source - buck controlled by the PDM pattern - Equivalent RL load association (Fig. 4).

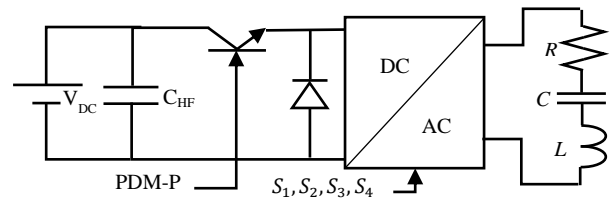


Fig. 3. Separation of the actions of modulation density et pulse generation

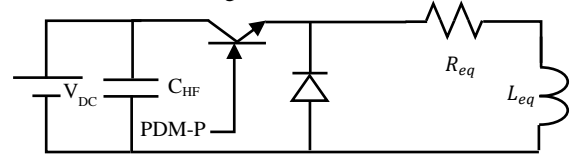


Fig. 4. PDM Inverter seen from DC side

## 4. PV Fed PDM Inverter

### A. Characterization process

We consider that the inverter is powered by a photovoltaic generator. During the active sequence of the PDM pattern, the inductance is charged by the PV generator via the resistor (Fig. 5.a). This sequence is followed by the inactive sequence. During this sequence, the capacitor is charged by the PV generator and the inductance is discharged (Fig. 5.b). It appears that we are in the presence of a process that brings together two processes: a capacitive load method and an inductive load method.

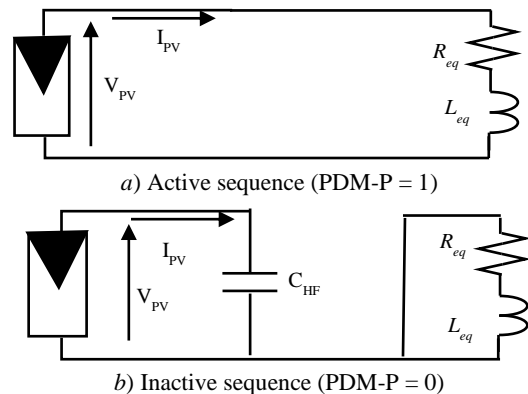


Fig. 5. Model of PV fed PDM inverter

### B. PDM pattern features

During the active sequence, the operating point of the PV panel describes the trajectory from the Open Circuit Point (OCP) to a Near Short Circuit Point (NSCP). The resistance  $R_{eq}$  prevents reaching the short-circuit point. But we remain very close to this point because  $R_{eq}$  assumes very low values by appropriate design. This makes it possible to trace the I-V characteristic in the OCP to Short Circuit Point (SCP) direction. This sequence must be long enough to fully charge the inductor. Assuming that the PV generator voltage remains constant and equal to  $V_{oc}$ , the minimum duration of the active sequence is then:

$$(\Delta T_{act})_{min} = L_{eq} I_{sc} / V_{oc} \quad (8)$$

During the inactive sequence, the operating point of the PV panel describes the trajectory from the short circuit point (SCP) to the open circuit point (OCP). This makes it possible to trace the I-V characteristic in the OCP to SCP

direction. This sequence must be long enough to fully charge the capacitor. Assuming that the PV generator current remains constant and equal to  $I_{sc}$ , the minimum duration of the inactive sequence is then:

$$(\Delta T_{inac})_{min} = C_{HF} V_{oc} / I_{sc} \quad (9)$$

Taking into account

$$\Delta T_{inac} = (1 - d)k / F_{res} \quad (10)$$

$$\Delta T_{acti} = d.k / F_{res} \quad (11)$$

(8) and (9) lead:

$$L_{eq} F_{res} I_{sc} / V_{oc} \leq d.k \leq k - C_{HF} F_{res} V_{oc} / I_{sc} \quad (12)$$

(12) leads:

$$L_{eq} F_{res} \frac{I_{sc}}{V_{oc}} + C_{HF} F_{res} \frac{V_{oc}}{I_{sc}} \leq k \quad (13)$$

If we want the proposed solution to be able to trace the characteristic under climatic conditions inducing short-circuit and open-circuit voltage variations in the intervals  $[(I_{sc})_{min} (I_{sc})_{max}]$  and  $[(V_{oc})_{min} (V_{oc})_{max}]$ , (12) and (13) become:

$$\frac{(I_{sc})_{max}}{(V_{oc})_{min}} L_{eq} F_{res} \leq d.k \leq k - \frac{(V_{oc})_{max}}{(I_{sc})_{min}} C_{HF} F_{res} \quad (14)$$

$$L_{eq} F_{res} \frac{(I_{sc})_{max}}{(V_{oc})_{min}} + C_{HF} F_{res} \frac{(V_{oc})_{max}}{(I_{sc})_{min}} \leq k \quad (15)$$

Equations (14) and (15) represent the constraints that the PDM pattern characteristics must satisfy.

## 5. Potential advancements of the proposed method

Compared to capacitive and inductive load methods, the proposed method combines the two and avoids their conceptual limitation. Indeed, these two methods present a conceptual limitation which lies in the fact that they are not continuously operational. In the case of a capacitive load method, the I-V curve is plotted when the capacitor is charging. The I-V curve cannot be plotted again until the capacitor is discharged. During the duration of the capacitor discharge, the I-V tracer based on capacitive load method is not operational. Similarly, tracers based on inductive load method are not operational during the inductor discharge phase. The proposed method is continuously operational.

Compared to methods based on DC-DC converters, the proposed method presents three specificities. The first specificity is that the switching is lossless. An impact of this specificity is that one can consider very high switching frequencies and therefore reduce the values of the inductance and the capacitance of the RLC load (R is the parasitic resistance). Reducing the value of the inductor implies reducing its parasitic resistance (R) and  $R_{eq}$ . The reduction induced in  $R_{eq}$  is slightly greater when the damping factor does not exceed 0.4 (Fig. 2). So if  $R_{eq}$  is low because  $L$  is low, the NSCP approaches the SCP. This first specificity may be a key for the proposed method to be able to trace the entire I-V characteristic. Another impact of this specificity is that the proposed method can be very fast. For example, if the switching frequency is 100 kHz and the pattern length  $k = 20$ , the IV curve is drawn in both directions in 200  $\mu$ s.

The second specificity is that the electronic power converter acts as a DC inductance emulator. The physical inductor is an HF inductor. Compared with a DC inductor of the same value, an AC inductor has a lower magnetic reluctance and a shorter electrical winding. The parasitic resistance and the emulated resistance are therefore lower (in case the winding

is made with Litz wire). Also, these resistances do not increase with the current of the PV generator. This is not the case with DC inductor used in DC-DC converters. It results then that the increase in the power of the PV Generator does not cause an increase in the weight, the volume and the parasitic resistance of the inductor used in the proposed solution.

The third specificity is that to trace the I-V curve the operating point of the converter remains invariant.

In the case of a tracer based on a DC-DC converter, to trace the IV curve of a PV generator under shading, the duty cycle of a DC-DC converter must sweep the interval [0 1] with a high resolution, which makes the tracer slower, if not with an adaptive step, which makes tracer control more complex. This problem is not applicable in the case of the proposed method.

The rapidity mentioned above does not refer to the tracer's ability to follow variations in the producible PV generator due to variations in climatic conditions. The rapidity in question refers to the ability of the tracer not to disturb PV production systems. All the methods cited in this work require the disconnection of the PV G from the production system for the time necessary to trace the IV curve. This time must be as short as possible to attenuate the effect of the disturbance. A tracer based on a DC-DC converter whose switching frequency is 20 kHz (common and reasonable value) needs 5 ms to trace the IV curve. 5 ms is a quarter of the 50 Hz grid period. Disconnecting a grid-connected PV system for a quarter of the period is a major disturbance. In the case of the proposed method with  $k = 20$  and  $F_{res} = 100$  kHz, the work is done in 100  $\mu$ s, i.e. 1% of the period of the 50 Hz grid. The disturbance is small and can be corrected.

## 6. Simulation and Experimental Results

The PV generator tested consists of 4 panels in series (ET-P636135) with  $V_{oc} = 4 \times 21.96 V = 87.84 V$ ,  $I_{sc} = 8.41 A$  and  $P_{max} = 4 \times 135 W = 540 W$  in STC. The chosen RLC resonant load is  $[C= 90$  nF,  $L= 20$   $\mu$ H]. R is estimated at 2  $\Omega$ . We calculate the switching frequency:  $F_{Swi} = F_{res} = 118$  kHz. Equations (6) and (7) lead:

$$L_{eq} = 49.3 \mu H \quad (16)$$

$$R_{eq} = 2.47 \Omega \quad (17)$$

We make the choice  $C_{HF} = 5.4 \mu F$ , and we fix:

$$(I_{sc})_{min} = 4 A \text{ and } (I_{sc})_{max} = 9 A \quad (18)$$

$$(V_{oc})_{min} = 84 V \text{ and } (V_{oc})_{max} = 86 V \quad (19)$$

Considering these data, (15) yields:

$$14,17 \leq k \quad (20)$$

We choose

$$k = 32 \quad (21)$$

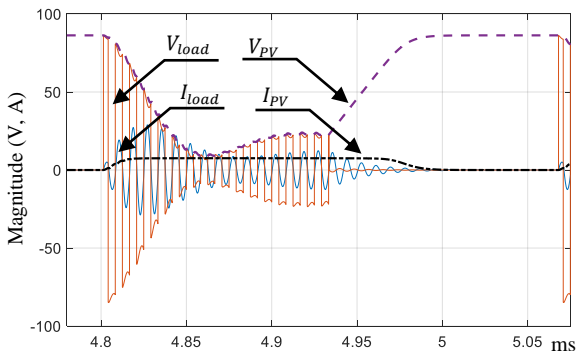
Considering all these data, (14) yields:

$$0.019 \leq d \leq 0.576 \quad (22)$$

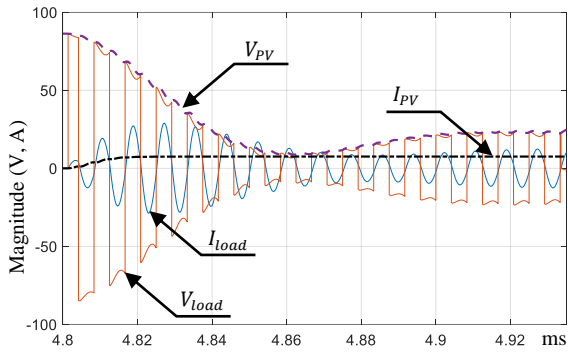
We choose

$$d = 16/32 \quad (23)$$

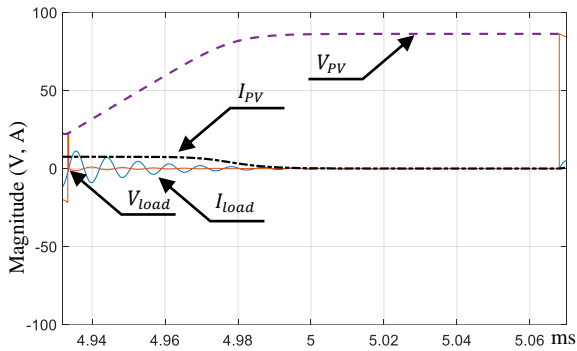
To check the feasibility of the proposed method and validate the design, simulations have been carried out in the Matlab-Simscape environment. Fig. 6 and 7 show the currents and voltages at the output and input of PDM inverter and the I-V curves for various irradiance values. The simulation results fully support the expected results.



a) Global view



b) During the active sequence of PDM pattern



c) During the inactive sequence of PDM pattern

Fig.6. Currents and voltages at the output and input of PDM inverter

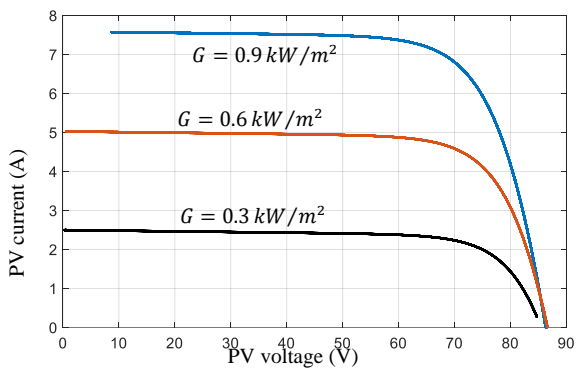
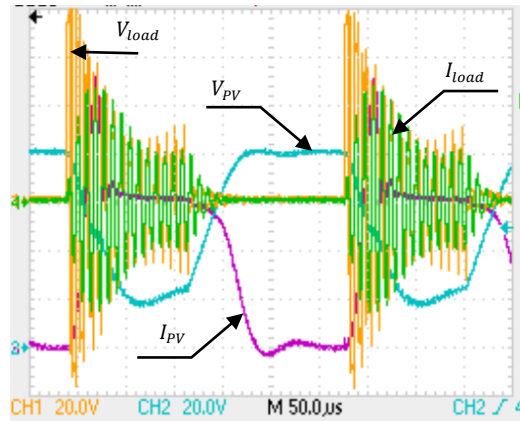


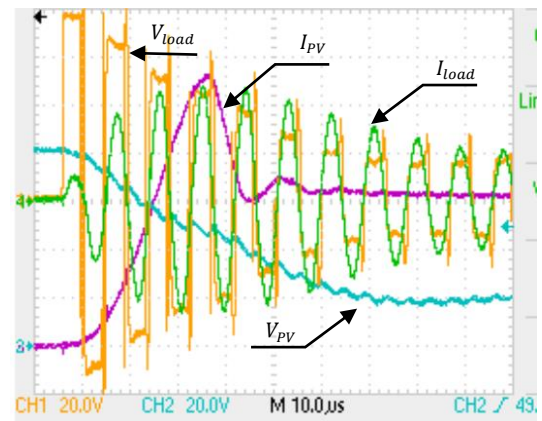
Fig.7. IV Curves – Simulation results

A first laboratory prototype corresponding to the simulated model is built. Fig. 8 shows an example of RLC load and PV panel currents and voltages. Fig. 9 shows the current and voltage of the PV generator in the case of the PDM pattern calculated above ( $k = 32$  and  $d = 16/32$ ). Fig. 10 shows the instantaneous I-V characteristic of the PV generator using the XY mode of the oscilloscope. In fig. 8, we observe

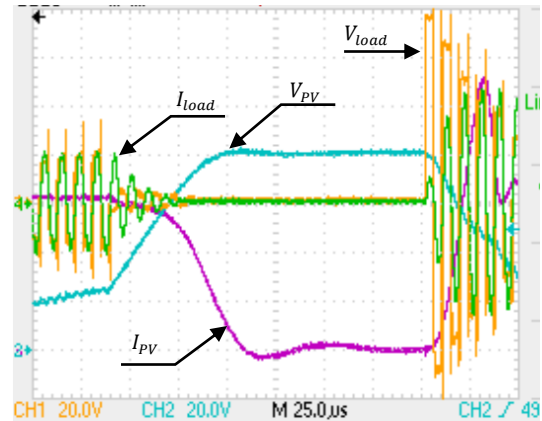
that at the beginning of the active PDM sequence, the current increases rapidly with a strong overshoot. This current overshoot is characteristic of a capacitive behavior of the photovoltaic generator. It shows the interest of a dynamic modeling of photovoltaic generators



a) Global view



b) During the active sequence of PDM pattern



c) During the inactive sequence of PDM pattern

Fig.8. Currents and voltages of RLC load and PV panel

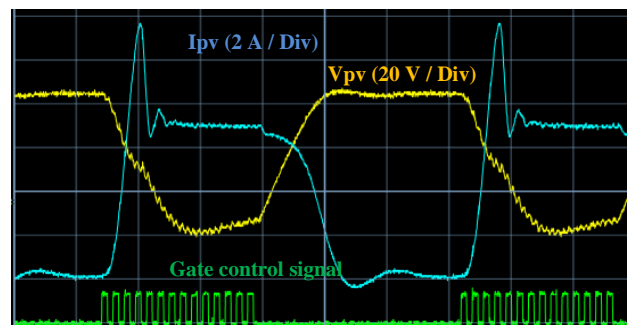


Fig.9. Current and voltage of PV panel

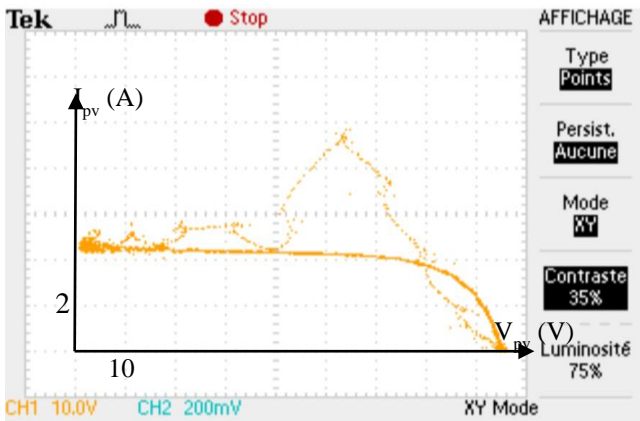


Fig.10. Example of I-V curve of PV panel

Tests under shade are carried out to test the effectiveness of the prototype built (Fig. 11). The result is satisfactory.

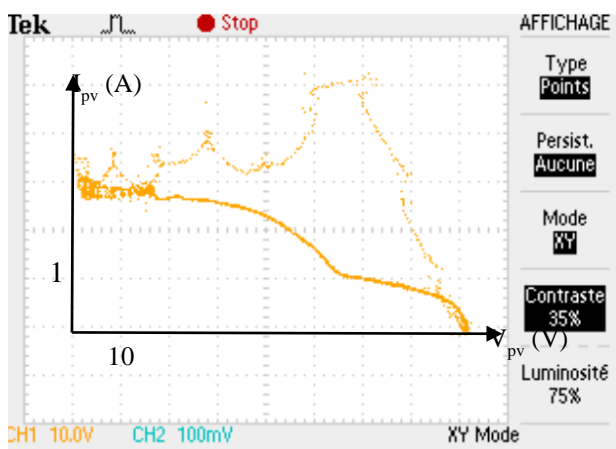


Fig.11. I-V curve of PV panel under shade

## 7. Conclusion and perspectives

A new solution for the PV panel characterization is presented. Instead of DC-DC converters, a DC-AC converter is chosen for this purpose: A PDM Inverter. The PDM inverter requires twice more semiconductor devices as most DC-DC converters. However, this disadvantage is compensated by advantages such as i) Very high switching frequencies are possible because switching is lossless. This makes it possible to reduce the measurement time of the characteristics; ii) The reactive components (inductor and capacitor) have very low values and/or operate in ac conditions and No DC inductor is required.; iii) The control circuit is very simple. Indeed, the duty cycle remains constant during the characterization. To check the feasibility and efficiency of the suggested solution, a laboratory prototype is built and the experimental results are presented.

## References

- [1] "Evolution of solar PV module cost by data source, 1970-2020" available on [www.iea.org/data-and-statistics/charts/evolution-of-solar-pv-module-cost-by-data-source-1970-2020](http://www.iea.org/data-and-statistics/charts/evolution-of-solar-pv-module-cost-by-data-source-1970-2020)
- [2] "Snapshot of Global PV Markets 2021", available on [https://iea-pvps.org/wp-content/uploads/2021/04/IEA\\_PVPS\\_Snapshot\\_2021-V3.pdf](https://iea-pvps.org/wp-content/uploads/2021/04/IEA_PVPS_Snapshot_2021-V3.pdf)
- [3] IEA (2021), Solar PV, IEA, Paris <https://www.iea.org/reports/solar-pv>
- [4] Global Energy review 2021, page 26, available on [www.iea.org](http://www.iea.org).
- [5] <https://www.pv-magazine.com/2022/03/15/humans-have-installed-1-terawatt-of-solar-capacity>
- [6] Net Zero by 2050 A Roadmap for the Global Energy available on <https://iea.blob.core.windows.net>.
- [7] IRENA (2019), Future of Solar Photovoltaic: Deployment, investment, technology, grid integration and socio-economic aspects (A Global Energy Transformation: paper), International Renewable Energy Agency, Abu Dhabi
- [8] I. M. Peters and P. Sinha, "Value of stability in photovoltaic life cycles," 2021 IEEE 48th Photovoltaic Specialists Conference (PVSC), 2021, pp. 0416-0419
- [9] Kim, J.; Rabelo, M.; Padi, S.P.; Yousuf, H.; Cho, E.-C.; Yi, J. A Review of the Degradation of Photovoltaic Modules for Life Expectancy. *Energies* 2021, 14, 4278.
- [10] R. E. Campos, E. Y. Sako, M. V. G. d. Reis and M. G. Villalva, "A Review of the Main Methods to trace the I-V Characteristic Curve of PV Sources," 2018 13th IEEE International Conference on Industry Applications (INDUSCON), 2018, pp. 24-30
- [11] E. A. Bastos, C. Meira Amaral da Luz, T. M. Oliveira, L. Ana Rodarte Rios, E. M. Vicente and F. Lessa Tofoli, "A Curve Tracer for Photovoltaic Modules Based on The Capacitive Load Method," 2019 IEEE 15th Brazilian Power Electronics Conference and 5th IEEE Southern Power Electronics Conference (COBEP/SPEC), Santos, Brazil, 2019, pp. 1-6,
- [12] Morales-Aragonés, J.I.; Dávila-Sacoto, M.; González, L.G.; Alonso-Gómez, V.; Gallardo-Saavedra, S.; Hernández-Callejo, L. A Review of I-V Tracers for Photovoltaic Modules: Topologies and Challenges. *Electronics* 2021, 10, 1283. <https://doi.org/10.3390/electronics10111283>
- [13] E. Durán, J. M. Andújar, J. M. Enrique, J. M. Pérez-Oria, "Determination of PV Generator I-V/P-V Characteristic Curves Using a DC-DC Converter Controlled by a Virtual Instrument", *International Journal of Photoenergy*, vol. 2012, Article ID 843185, 13 pages, 2012.
- [14] N. Saini, A. Mudgal, K. Kumar, J. Srivastava and V. Dutta, "Design of microcontroller based I-V plotter using IGBT electronic load," 2016 IEEE 1st International Conference on Power Electronics, Intelligent Control and Energy Systems (ICPEICES), 2016, pp. 1-5
- [15] W. Sirichote, C. Wuttikornkanarak, S. Srathongkao, S. Suttiyan, N. Somdock and B. Klongratog, "IV Tracer For Photovoltaic Panel," 2021 7th International Conference on Engineering, Applied Sciences and Technology (ICEAST), 2021, pp. 54-57
- [16] V. Boscaino, G. Cipriani, V. Di Dio, R. Miceli, G. Prestigiacomo and A. Pulizzotto, "A DC-DC power converter for PV module characterization," 2014 International Symposium on Power Electronics, Electrical Drives, Automation and Motion, 2014, pp. 998-1002
- [17] H. Fujita and H. Akagi, "Pulse-density-modulated power control of a 4 kW, 450 kHz voltage-source inverter for induction melting applications," in *IEEE Transactions on Industry Applications*, vol. 32, no. 2, pp. 279-286, March-April 1996
- [18] A. Sandali, A. Cheriti, P. Sicard and K. Al-Haddad, "Application of PDM control to a multilevel AC/AC converter with self power factor correction," 2004 IEEE 35th Annual Power Electronics Specialists Conference (IEEE Cat. No.04CH37551), 2004, pp. 2881-2887 Vol.4
- [19] A. Sandali, A. Cheriti and P. Sicard, "PDM Ac/ac converter with three-phase diode rectifier including power factor correction," 2008 IEEE International Symposium on Industrial Electronics, 2008, pp. 347-352
- [20] A. Sandali and A. Cheriti, .." Pulse Density Modulation Applied to Series Resonant Inverter and Ac - Ac Conversion" Chapter 4 in *Recent Developments on Power Inverters book*, Edited by Ali Saghafinia, ISBN 978-953-51-3232-5, Print ISBN 978-953-51-3231-8, Publisher: InTech, June 21, 2017 DOI: 10.5772/65189.